

# Simplified protein design biased for prebiotic amino acids yields a foldable, halophilic protein

Liam M. Longo, Jihun Lee<sup>1</sup>, and Michael Blaber<sup>2</sup>

Department of Biomedical Sciences, Florida State University, Tallahassee, FL 32306-4300

Edited by Brian W. Matthews, University of Oregon, Eugene, OR, and approved December 19, 2012 (received for review November 9, 2012)

**A compendium of different types of abiotic chemical syntheses identifies a consensus set of 10 “prebiotic”  $\alpha$ -amino acids. Before the emergence of biosynthetic pathways, this set is the most plausible resource for protein formation (i.e., proteogenesis) within the overall process of abiogenesis. An essential unsolved question regarding this prebiotic set is whether it defines a “foldable set”—that is, does it contain sufficient chemical information to permit cooperatively folding polypeptides? If so, what (if any) characteristic properties might such polypeptides exhibit? To investigate these questions, two “primitive” versions of an extant protein fold (the  $\beta$ -trefoil) were produced by top-down symmetric deconstruction, resulting in a reduced alphabet size of 12 or 13 amino acids and a percentage of prebiotic amino acids approaching 80%. These proteins show a substantial acidification of pI and require high salt concentrations for cooperative folding. The results suggest that the prebiotic amino acids do comprise a foldable set within the halophile environment.**

protein simplification | protein evolution

**P**roteins play a central role in the metabolic processes that enable living systems; thus, proteogenesis (the origin of proteins) is a key event within the grander process of abiogenesis (the origin of life from nonliving matter). Strikingly, the majority of studies designed to reproduce abiotic chemical syntheses in the early Earth, as well as compositional analyses of comets and meteorites (pristine remnants of the early solar system), report the significant presence of  $\alpha$ -amino and  $\alpha$ -carboxylic acids—and with typically greater abundance than nucleobases or riboses [for a recent review see ref. (1)]. A consensus set of prebiotic amino acids has emerged from a compendium of such studies and comprises Ala, Asp, Glu, Gly, Ile, Leu, Pro, Ser, Thr, and Val (1–3). The close correspondence between spark discharge-type experiments, thermal vent chemistry, and analyses of comets and meteorites suggests a possible common synthetic mechanism, such as Strecker synthesis (4–6).

Before the establishment of biosynthetic pathways yielding novel amino acids, the first polypeptides were likely composed only of those amino acids freely available in the environment (the prebiotic set). In a “protein-first” view of abiogenesis, the prebiotic set of amino acids possesses properties sufficient and necessary to permit the emergence of polypeptides capable of supporting simple metabolic or biosynthetic reactions. One of the most fundamental yet demanding properties of such polypeptides is the ability to support cooperative folding, such that defined structure (and a concomitant functionality) is possible with the earliest polypeptides. Stated differently, a key question for proteogenesis is whether the set of prebiotic amino acids is capable of providing a solution to the Levinthal paradox (7). Viewed in terms of this requirement, the prebiotic set is remarkable in containing high-propensity amino acids for each of the basic types of protein secondary structure (8–11) as well as hydrophobic and hydrophilic amino acids with the potential to support patterning essential for specific secondary and tertiary structure organization (12, 13); furthermore, the prebiotic set contains amino acids capable of functioning as catalytic nucleophiles. However, the barrier to prebiotic protein folding appears steep, as the characteristics of a purely prebiotic protein present a stark deviation from the majority of extant proteins, because: (i) the prebiotic amino acid alphabet contains only 10 letters, thereby

reducing the potential diversity of interactions that can be encoded to that of currently proposed theoretic limits for foldability (14–16) (thus, to be able to support protein foldability, the 10 prebiotic amino acids would need to be a remarkably efficient selection); (ii) aromatic residues, key contributors to extensive van der Waals interactions in hydrophobic cores that serve as a driving force for protein collapse, are absent in the prebiotic alphabet; and (iii) there are no basic amino acids in the prebiotic set, thus restricting protein design to acidic polypeptides, limiting the presence of salt bridge interactions and resulting in acidic pI (1, 3).

To date, there has been no experimental demonstration that the prebiotic set of amino acids comprises a foldable set; additionally, there has been no elucidation of any intrinsic property of a polypeptide constructed from the prebiotic set. Recent “top-down” protein design studies have successfully identified relatively small peptide building blocks (i.e., 40–50 amino acids) capable of spontaneous assembly into common symmetric protein folds, and in the process, support plausible evolutionary pathways starting from simple peptide motifs and traversing foldable sequence space [for a review see ref. (17)]. A simplified  $\beta$ -trefoil protein (*Symfoil-4P*) having a reduced amino acid alphabet size of 16 letters, and enriched in prebiotic amino acids (to 71%), was constructed in our laboratory using the top-down symmetric deconstruction method (18). Using this simplified  $\beta$ -trefoil protein as a departure point, two “primitive”  $\beta$ -trefoil proteins, (PV1 and PV2 for primitive version 1 and 2, respectively) were constructed with reduced amino acid alphabets and further enrichment of prebiotic amino acids. The PV1 and PV2 proteins reduce the alphabet size to 13 and 12 amino acids, respectively. Notably, the entire core region (involving a total of 21 amino acid positions) in PV2 is reduced to an alphabet of only three amino acids and is entirely prebiotic. Enrichment for the exclusively acidic prebiotic alphabet subsequently increases the negative charge bias, and PV1 and PV2 have pI values and surface electrostatic charge distributions typical of halophilic proteins. Stability studies demonstrate a significant halophilic property, especially for PV2 (which is shown to be an obligate halophile). Our experimental results provide support for the hypothesis that the prebiotic set of amino acids defines a foldable set and, furthermore, that such foldability is most compatible with the halophile environment.

## Results

**Mutant Sequence Characteristics.** PV1 and PV2 (Fig. 1) comprise a reduced set of amino acids (13 and 12 amino acid alphabet size,

Author contributions: L.M.L., J.L., and M.B. designed research; L.M.L. and J.L. performed research; L.M.L., J.L., and M.B. analyzed data; and L.M.L., J.L., and M.B. wrote the paper.

The authors declare no conflict of interest.

This article is a PNAS Direct Submission.

Data deposition: The atomic coordinates and structures factors reported in this paper have been deposited in the Protein Data Bank, [www.pdb.org](http://www.pdb.org) (PDB ID codes 3Q7W, 3Q7X, and 4D8H).

<sup>1</sup>Present address: Celltrion Inc., Yeonsu-gu, Incheon City 406-840, Korea.

<sup>2</sup>To whom correspondence should be addressed. E-mail: michael.blaber@med.fsu.edu.

This article contains supporting information online at [www.pnas.org/lookup/suppl/doi:10.1073/pnas.1219530110/-DCSupplemental](http://www.pnas.org/lookup/suppl/doi:10.1073/pnas.1219530110/-DCSupplemental).

FGF-1 15 20 25 30 35 40 45 50 52  
 PKLLLYC S N G G . . . H F L R I L P D G T V D G . . . T R D R S D Q H I Q L Q L S A E S V G  
 55 60 65 70 75 80 85 90 93  
 E V Y I K S T E T G . . . Q Y L A M D T D G L L Y G . . . S Q T P N E E C L F L E R L E E N H  
 95 100 105 110 115 120 125 130 135 140  
 Y N T Y I S K K H A E K N W F V G L K K N G S C K R G R T H Y G Q K A I L F L P L P V S S D

*Symfoi*-4P  
 15 20 25 30 35 40 45 50 52  
 P V L L K S T E T G Q Y L R I N P D G T V D G T R D R S D P H I Q F Q I S P E G N G  
 55 60 65 70 75 80 85 90 93  
 E V L L K S T E T G Q Y L R I N P D G T V D G T R D R S D P H I Q F Q I S P E G N G  
 95 100 103107 110 115 119123 125 130 135 140  
 E V L L K S T E T G Q Y L R I N P D G T V D G T R D R S D P H I Q F Q I S P E G N G

PV1  
 15 20 25 30 35 40 45 50 52  
 E V L L R S T E T G Q F L R I N P D G T V D G T R D R S D P G I Q F Q I S P E G N G  
 55 60 65 70 75 80 85 90 93  
 E V L L R S T E T G Q F L R I N P D G T V D G T R D R S D P G I Q F Q I S P E G N G  
 95 100 103107 110 115 119123 125 130 135 140  
 E V L L R S T E T G Q F L R I N P D G T V D G T R D R S D P G I Q F Q I S P E G N G

PV2  
 15 20 25 30 35 40 45 50 52  
 E V L L R S T E T G Q L L R I N P D G T V D G T R D R S D P G I Q L Q I S P E G N G  
 55 60 65 70 75 80 85 90 93  
 E V L L R S T E T G Q L L R I N P D G T V D G T R D R S D P G I Q L Q I S P E G N G  
 95 100 103107 110 115 119123 125 130 135 140  
 E V L L R S T E T G Q L L R I N P D G T V D G T R D R S D P G I Q L Q I S P E G N G

**Fig. 1.** Amino acid sequence of FGF-1, *Symfoi*-4P, PV1, and PV2 mutants (single letter code). The sequences are aligned by the threefold axis of rotational symmetry internal to the  $\beta$ -trefoil fold (i.e., each line is one trefoil-fold repeat element within the overall  $\beta$ -trefoil structure). The numbering of *Symfoi*-4P, PV1, and PV2 amino acids is based upon corresponding positions in FGF-1. The shaded positions identify amino acids belonging to the prebiotic set.

respectively) and biased for the prebiotic alphabet (74% and 79% prebiotic, respectively) (Fig. 2). PV1 contains six aromatic amino acids: three Phe residues within the central hydrophobic core (positions 44, 85, and 132) and an additional three within isolated “minicore” regions (positions 22, 64, and 108) (19). In PV2, all six buried Phe residues have been mutated to Leu to generate a protein devoid of aromatic residues. In contrast to FGF-1 (which has a charge bias of +5 and a pI of 7.88), the *Symfoi*-4P protein is more acidic (charge bias  $-5$  and pI of 4.70) (Fig. 2). PV1 and PV2 substantially extend such acidity (charge bias  $-9$  and pI 4.36, in both cases) in response to the acidic bias of the prebiotic set. Despite the amino acid compositional changes resulting from the restrictions of the prebiotic alphabet, plots of  $\beta$ -sheet propensity,  $\beta$ -turn propensity, and hydrophobicity for FGF-1, PV1, and PV2 show that PV1 and PV2 preserve the essential secondary structure and hydrophobic-polar patterning characteristics intrinsic to the  $\beta$ -trefoil architecture (Fig. S1).

**X-Ray Crystallography.** Both PV1 and PV2 produced diffraction-quality crystals, and all crystals grew from 1.5 M ammonium sulfate,  $\sim 0.1$  M lithium sulfate, and 0.1 M Tris buffer pH 7.0–7.4 (Table S1). Global differences between the structures of PV1 and PV2 are small, as demonstrated by a  $C\alpha$  rmsd of 0.38 Å. Structural perturbations near the sites of mutation are largely restricted to minor movement of local side chains [ $C\alpha$  rmsd values within 4.5 Å ( $\sim 12$  residues) of the mutation sites are  $<0.3$  Å]. An overlay of PV1 or PV2 onto *Symfoi*-4P yields  $C\alpha$  rmsd values of 0.5–0.6 Å, indicating general structural conservation in response to the increase in prebiotic amino acids. The core region of the  $\beta$ -trefoil fold, including the main central core and the three peripheral minicores, comprises 21 positions (Fig. S2) (19, 20). In FGF-1, this group has an alphabet of seven types of amino acids, burying 96 carbons in total, and having 67% prebiotic amino acid composition (Fig. S3). The *Symfoi*-4P protein has a reduced core-packing alphabet size of five amino acids, resulting principally from the elimination of buried free thiols as well as elimination of an asymmetric secondary structure involving Met67 (18, 21). The *Symfoi*-4P core-packing group buries 99 carbons, or three more than the FGF-1 protein. However, compared with FGF-1, *Symfoi*-4P exhibits a significant

reduction in core-packing defects (due principally to the imposition of tertiary structure symmetry; Fig. S2). The *Symfoi*-4P core-packing group also increases the percentage of prebiotic amino acids of this region to 83%. The PV1 mutant reduces the core-packing alphabet size further to four amino acids and, compared with *Symfoi*-4P, has no reduction in total number of carbons, has an essentially equivalent core-packing efficiency, and has an unchanged percentage of core prebiotic amino acids (83%). In contrast, the PV2 mutant core packing is achieved with an alphabet size of only three amino acids (comprising Leu, Ile, and Val), and is exclusively prebiotic (Fig. S3). The PV2 core buries 81 carbons—a substantial reduction from the 99 in PV1. The calculated loss of side chain volume for a total of six Phe $\rightarrow$ Leu mutations is  $139 \text{ \AA}^3$  (22). The PV2 crystal structure (solved under high-salt conditions) shows that the protein cannot adjust completely to avoid packing defects—several cavities within the core of PV2 are detectable using  $1.2 \text{ \AA}$  probe radius, with a combined volume of  $57 \text{ \AA}^3$  (Fig. S2).

**Differential Scanning Calorimetry.** Stability studies using differential scanning calorimetry (DSC) were performed in both low (0.1 M) and high (2.0 M; i.e., 33% saturated) NaCl solutions. Both conditions provide sufficient ionic strength to screen electrostatic interactions; thus, the differential salt stability evaluates Hofmeister effects. Thermal denaturation of FGF-1 in 0.1 M NaCl occurs concomitant with irreversible precipitation as evidenced by sharp exothermic signal subsequent to initial denaturation endotherm [resulting in large apparent negative  $\Delta C_p$  (constant pressure heat capacity)] and visible turbidity of the sample (23). Although soluble in 2.0 M NaCl, FGF-1 similarly precipitates upon thermal denaturation; however, 2.0 M NaCl stabilizes FGF-1 by  $\sim +16$  °C (as determined from the difference in apparent endotherm peak) (Table S2). *Symfoi*-4P is a hyperthermophile with a melting temperature of 85 °C in 0.1 M NaCl buffer. In the presence of 2.0 M

Amino Acid	FGF-1	<i>Symfoi</i> -4P	PV1	PV2
A	4			
C	3			
D	7	12	12	12
E	8	8	9	9
F	4	3	6	
G	12	15	18	18
H	5	3		
I	5	9	9	9
K	9	3		
L	16	9	9	15
M	1			
N	6	6	6	6
P	6	10	9	9
Q	6	9	9	9
R	6	9	12	12
S	10	9	9	9
T	8	12	12	12
V	5	6	6	6
W	1			
Y	7	3		
Alphabet size	20	16	13	12
Charge bias	+5	-5	-9	-9
pI	7.88	4.70	4.36	4.36
Aromatic res.	12	6	6	0
% Pre-biotic	62	71	74	79

**Fig. 2.** Amino acid composition of FGF-1, *Symfoi*-4P, PV1, and PV2 mutants. Also shown are the alphabet size, charge bias, pI, number of aromatic residues, and % prebiotic amino acids for each protein. The shaded positions identify amino acids belonging to the prebiotic set.



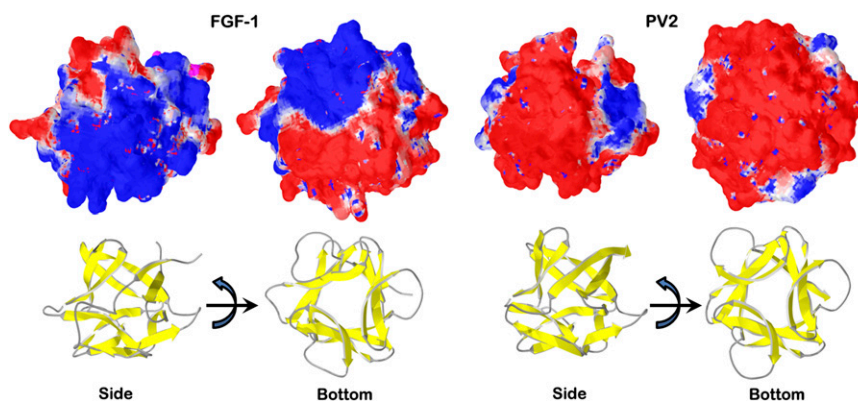


**Fig. 4.** Surface electrostatic charge distribution of FGF-1 and PV2 proteins. Beneath each surface representation is an associated ribbon diagram in the same orientation. The left-most image of each pair is a side view; the right-most image is rotated 90° about the horizontal axis to provide a bottom view of the overall  $\beta$ -barrel structure. Positive charge density is indicated by blue, and negative by red. The (a)symmetric features of each protein can be appreciated in the right-most (bottom) view in each case. The acidic nature of the prebiotic set of amino acids is evident with the enrichment of such residues in the PV2 protein.

acids belonging to the prebiotic set (Fig. 2). The least frequent residues in *Symfoi-4P* (with single examples at threefold symmetry-related positions) include Phe, His, Lys, and Tyr residues.

For PV1, the goal was to reduce the alphabet further to 13 amino acids and enrich for prebiotic amino acids by substituting all Lys residues (positions 15, 57, and 98) to Arg (alphabet reduction), substituting all Tyr residues (positions 22, 64, and 108) to Phe (alphabet reduction), and substituting all His residues (positions 41, 82, and 129) to Gly (prebiotic enrichment). The Lys→Arg and Tyr→Phe substitutions were considered conservative substitutions with likelihood of minimum structural perturbation. The His→Gly mutations occur within a solvent-exposed turn position in which Gly is a common residue (35). Overall, the design of PV1 involved a significant reduction in alphabet size (from 16 to 13 amino acids) combined with an increase in fraction of prebiotic amino acids from 71% (*Symfoi-4P*) to 74% (Fig. 2).

The primary design goal for PV2 was to create an entirely prebiotic core-packing group at the 21 buried positions in the  $\beta$ -trefoil fold, with further reduction in alphabet size and increase in fraction of prebiotic amino acids compared with PV1. The PV2 protein used PV1 as a background and introduced either Leu, Ile, or Val mutations simultaneously at positions 22, 44, 64, 85, 108, and 132. These positions are all aromatic residues in *Symfoi-4P* (Phe and Tyr) and PV1 (Phe) (Fig. 1). Val mutations at these core positions resulted in a nonfolded and insoluble protein. Ile mutations yielded some soluble protein; however, the yield of soluble protein appeared notably higher with the Leu mutations; thus, Ile and Val mutations were not pursued further. Overall, the design of PV2 involved a further reduction in alphabet size compared with PV1 (from 13 to 12 amino acids) combined with an increase in fraction of prebiotic amino acids from

74% (PV1) to 79% (Fig. 2). Propensity plots for  $\beta$ -turn and  $\beta$ -sheet formation were calculated using values reported by Levitt (36) and Chou and Fasman (37), respectively.

**Protein Mutagenesis, Expression, and Purification.** Details of protein mutagenesis, expression and purification are provided in supplementary information.

**DSC.** All DSC data were collected on a VP-DSC microcalorimeter (GE Healthcare) as previously described (23). Briefly, 40  $\mu$ M protein samples in *N*-(2-acetamido)iminodiacetic acid buffer containing 0.1 M or 2.0 M NaCl were analyzed at a scan rate of 15 K/h. Triplicate runs were collected and molar heat capacity data were analyzed using the *DSCfit* software package (38).

**X-Ray Crystallography.** Details of protein crystallization and X-ray structure determination are provided in supplementary information. Model coordinates for the refined PV1 crystal form 1 (PDB ID code 3Q7W) and form 2 (PDB ID code 3Q7X) as well as PV2 (PDB ID code 4D8H) have been deposited in the Protein Data Bank.

**ACKNOWLEDGMENTS.** We thank Dr. Thayumanasamy Somasundaram for assistance with X-ray diffraction data collection and analysis. Use of the National Synchrotron Light Source, Brookhaven National Laboratory, is also acknowledged. This work was supported by the Office of Biological and Environmental Research and the Office of Basic Energy Sciences of the US Department of Energy and the National Center for Research Resources of the National Institutes of Health.

- Longo LM, Blaber M (2012) Protein design at the interface of the pre-biotic and biotic worlds. *Arch Biochem Biophys* 526(1):16–21.
- Doi N, Kakukawa K, Oishi Y, Yanagawa H (2005) High solubility of random-sequence proteins consisting of five kinds of primitive amino acids. *Protein Eng Des Sel* 18(6): 279–284.
- McDonald GD, Storrle-Lombardi MC (2010) Biochemical constraints in a protobiotic earth devoid of basic amino acids: The “BAA(-) world.” *Astrobiology* 10(10):989–1000.
- Huber C, Wächtershäuser G (2006)  $\alpha$ -Hydroxy and  $\alpha$ -amino acids under possible Hadean, volcanic origin-of-life conditions. *Science* 314(5799):630–632.
- Lerner NR, Peterson E, Chang S (1993) The Strecker synthesis as a source of amino acids in carbonaceous chondrites: Deuterium retention during synthesis. *Geochim Cosmochim Acta* 57(19):4713–4723.
- Wolman Y, Haverland WJ, Miller SL (1972) Nonprotein amino acids from spark discharges and their comparison with the Murchison meteorite amino acids. *Proc Natl Acad Sci USA* 69(4):809–811.
- Levinthal C (1969) How to fold graciously. *Mossbauer Spectroscopy in Biological Systems*, eds DeBrunner JTP, Munck E (Univ of Illinois Press, Champaign, IL) pp 22–24.
- Pace CN, Scholtz JM (1998) A helix propensity scale based on experimental studies of peptides and proteins. *Biophys J* 75(1):422–427.
- Street AG, Mayo SL (1999) Intrinsic beta-sheet propensities result from van der Waals interactions between side chains and the local backbone. *Proc Natl Acad Sci USA* 96(16):9074–9076.
- Gunasekaran K, Ramakrishnan C, Balaram P (1997) Beta-hairpins in proteins revisited: Lessons for *de novo* design. *Protein Eng* 10(10):1131–1141.
- Hutchinson EG, Thornton JM (1994) A revised set of potentials for beta-turn formation in proteins. *Protein Sci* 3(12):2207–2216.
- Xiong H, Buckwalter BL, Shieh HM, Hecht MH (1995) Periodicity of polar and nonpolar amino acids is the major determinant of secondary structure in self-assembling oligomeric peptides. *Proc Natl Acad Sci USA* 92(14):6349–6353.
- Bellesia G, Jewett AI, Shea JE (2010) Sequence periodicity and secondary structure propensity in model proteins. *Protein Sci* 19(1):141–154.
- Fan K, Wang W (2003) What is the minimum number of letters required to fold a protein? *J Mol Biol* 328(4):921–926.
- Murphy LR, Wallqvist A, Levy RM (2000) Simplified amino acid alphabets for protein fold recognition and implications for folding. *Protein Eng* 13(3):149–152.
- Romero P, Obradovic Z, Dunker AK (1999) Folding minimal sequences: The lower bound for sequence complexity of globular proteins. *FEBS Lett* 462(3):363–367.
- Blaber M, Lee J (2012) Designing proteins from simple motifs: Opportunities in top-down symmetric deconstruction. *Curr Opin Struct Biol* 22(4):442–450, 10.1016/j.sbi.2012.05.008.
- Lee J, Blaber SI, Dubey VK, Blaber M (2011) A polypeptide “building block” for the  $\beta$ -trefoil fold identified by “top-down symmetric deconstruction.” *J Mol Biol* 407(5): 744–763.
- Dubey VK, Lee J, Blaber M (2005) Redesigning symmetry-related “mini-core” regions of FGF-1 to increase primary structure symmetry: Thermodynamic and functional consequences of structural symmetry. *Protein Sci* 14(9):2315–2323.
- Blaber M, DiSalvo J, Thomas KA (1996) X-ray crystal structure of human acidic fibroblast growth factor. *Biochemistry* 35(7):2086–2094.
- Lee J, Blaber M (2011) Experimental support for the evolution of symmetric protein architecture from a simple peptide motif. *Proc Natl Acad Sci USA* 108(1): 126–130.
- Zamyatin AA (1972) Protein volume in solution. *Prog Biophys Mol Biol* 24:107–123.

23. Blaber SI, Culajay JF, Khurana A, Blaber M (1999) Reversible thermal denaturation of human FGF-1 induced by low concentrations of guanidine hydrochloride. *Biophys J* 77(1):470–477.
24. Collins KD, Washabaugh MW (1985) The Hofmeister effect and the behaviour of water at interfaces. *Q Rev Biophys* 18(4):323–422.
25. Broering JM, Bommarius AS (2005) Evaluation of Hofmeister effects on the kinetic stability of proteins. *J Phys Chem B* 109(43):20612–20619.
26. Zhang Y, Cremer PS (2006) Interactions between macromolecules and ions: The Hofmeister series. *Curr Opin Chem Biol* 10(6):658–663.
27. Vonhippel PH, Wong K-Y (1964) Neutral salts: The generality of their effects on the stability of macromolecular conformations. *Science* 145(3632):577–580.
28. Inouye K, Kuzuya K, Tonomura B (1998) Sodium chloride enhances markedly the thermal stability of thermolysin as well as its catalytic activity. *Biochim Biophys Acta* 1388(1):209–214.
29. Bágel'ová J, Fedunová D, Gazová Z, Fabian M, Antalík M (2008) Influence of NaCl and sorbitol on the stability of conformations of cytochrome c. *Biophys Chem* 135(1-3): 110–115.
30. Hutcheon GW, Vasisht N, Bolhuis A (2005) Characterisation of a highly stable  $\alpha$ -amylase from the halophilic archaeon *Haloarcula hispanica*. *Extremophiles* 9(6):487–495.
31. Paul S, Bag SK, Das S, Harvill ET, Dutta C (2008) Molecular signature of hypersaline adaptation: Insights from genome and proteome composition of halophilic prokaryotes. *Genome Biol* 9(4):R70.71-19.
32. Eisenberg H, Mevarech M, Zaccai G (1992) Biochemical, structural, and molecular genetic aspects of halophilism. *Adv Protein Chem* 43:1–62.
33. Kennedy SP, Ng WV, Salzberg SL, Hood L, DasSarma S (2001) Understanding the adaptation of *Halobacterium* species NRC-1 to its extreme environment through computational analysis of its genome sequence. *Genome Res* 11(10):1641–1650.
34. Oren A, Larimer F, Richardson P, Lapidus A, Csonka LN (2005) How to be moderately halophilic with broad salt tolerance: Clues from the genome of *Chromohalobacter salexigens*. *Extremophiles* 9(4):275–279.
35. Lee J, Dubey VK, Longo LM, Blaber M (2008) A logical OR redundancy within the Asx-Pro-Asx-Gly type I  $\beta$ -turn motif. *J Mol Biol* 377(4):1251–1264.
36. Levitt M (1978) Conformational preferences of amino acids in globular proteins. *Biochemistry* 17(20):4277–4285.
37. Chou PY, Fasman GD (1978) Prediction of the secondary structure of proteins from their amino acid sequence. *Adv Enzymol Relat Areas Mol Biol* 47:45–148.
38. Grek SB, Davis JK, Blaber M (2001) An efficient, flexible-model program for the analysis of differential scanning calorimetry protein denaturation data. *Protein Pept Lett* 8(6):429–436.

# Supporting Information

M. Longo et al. 10.1073/pnas.1219530110

## SI Materials and Methods

**Protein Expression and Purification.** Primitive version (PV)1 and PV2 mutants were constructed in the background of the de novo designed simplified  $\beta$ -trefoil protein (*Symfoil-4P*) synthetic gene (1). The constructs contained an additional amino-terminal (His)<sub>6</sub> tag but deleted residues 1–10 of the *Symfoil-4P* protein. These deleted residues are not part of the fundamental  $\beta$ -trefoil architecture but comprise an unstructured N-terminal extension and were deleted to promote crystallization and reduce the biotic amino acid composition. The numbering scheme of the FGF-1 protein is retained in the PV1 and PV2 mutants for purposes of comparison (Fig. 1). The QuikChange site-directed mutagenesis protocol (Agilent Technologies) was used to introduce all mutations, which were confirmed by nucleic acid sequence analysis (Biomolecular Analysis Synthesis and Sequencing Laboratory, Florida State University). Expression and purification of recombinant proteins followed previously published procedures (2) and used Ni-NTA chelation and Superdex 75 size-exclusion chromatography (GE Healthcare). Purified protein was exchanged into 50 mM sodium phosphate, 0.1 M NaCl, 10 mM (NH<sub>4</sub>)<sub>2</sub>SO<sub>4</sub>, pH 7.5 (“crystallization buffer”) for crystallization studies or 20 mM *N*-(2-acetamido)iminodiacetic acid (ADA), 0.1 M or 2.0 M NaCl, pH 6.6 (“ADA buffer”) for all biophysical studies. The extinction coefficients for FGF-1 and *Symfoil-4P* mutant form were determined by the method of Gill and von Hippel (3); concentration of PV1 and PV2 were determined by bicinchoninic acid assay in reference to a known *Symfoil-4P* (1, 4) concentration standard.

**X-Ray Crystallography.** Purified mutant protein in crystallization buffer was concentrated to 10–15 mg/mL and crystal screening was performed using either the hanging-drop or sitting-drop vapor diffusion method at room temperature. Two different orthorhombic crystal forms of the PV1 mutant grew from 1.5 M (NH<sub>4</sub>)<sub>2</sub>SO<sub>4</sub>, 0.10 M Li<sub>2</sub>SO<sub>4</sub>, and either 0.1 M Hepes pH 7.4 (form 1) or 0.1 M Tris pH 7.0 (form 2). An orthorhombic crystal form of the PV2 mutant grew from 1.5 M (NH<sub>4</sub>)<sub>2</sub>SO<sub>4</sub>, 0.11 M Li<sub>2</sub>SO<sub>4</sub>, 0.1 M Tris pH 7.0. Crystals were mounted using Hampton Research nylon mounted cryo-turns and cryo-cooled in a stream of gaseous nitrogen at 100 K. Diffraction data for both PV1 crystals were collected at the  $\times 25$  beam line of the National Synchrotron Light Source at Brookhaven National Laboratory using an ADSC Q315 CCD detector. Diffraction data for PV2 were collected in-house, using a Rigaku RU-H2R rotating anode X-ray source equipped with an Osmic confocal mirrors (MarUSA) and a MarCCD165 detector. A single-crystal diffraction dataset was collected in each case and diffraction data were indexed, integrated, and scaled using the DENZO or HKL2000 software package (5, 6). Molecular replacement and refinement used the PHENIX software package (7), with 5% of the data in the reflection files set aside for  $R_{\text{free}}$  calculations (8). The structure was solved by molecular replacement, in which the *Symfoil-4P* de novo designed protein [Protein Data Bank (PDB) IDcode 3O4D] was used as the search model for PV1; subsequently, PV1 was used as the search model for PV2. Model building and visualization used the COOT molecular graphics software (9).

1. Lee J, Blaber M (2011) Experimental support for the evolution of symmetric protein architecture from a simple peptide motif. *Proc Natl Acad Sci USA* 108(1): 126–130.
2. Brych SR, Blaber SI, Logan TM, Blaber M (2001) Structure and stability effects of mutations designed to increase the primary sequence symmetry within the core region of a  $\beta$ -trefoil. *Protein Sci* 10(12):2587–2599.
3. Gill SC, von Hippel PH (1989) Calculation of protein extinction coefficients from amino acid sequence data. *Anal Biochem* 182(2):319–326.
4. Lee J, Blaber SI, Dubey VK, Blaber M (2011) A polypeptide “building block” for the  $\beta$ -trefoil fold identified by “top-down symmetric deconstruction.” *J Mol Biol* 407(5):744–763.
5. Otwinowski Z (1993) Oscillation data reduction program. *Proceedings of the CCP4 Study Weekend: “Data Collection and Processing,”* eds Sawyer L, Isaacs N, Bailey S (SERC Daresbury Laboratory, Daresbury, England), pp 56–62.
6. Otwinowski Z, Minor W (1997) Processing of x-ray diffraction data collected in oscillation mode. *Methods Enzymol* 276(part A):307–326.
7. Zwart PH, et al. (2008) Automated structure solution with the PHENIX suite. *Methods Mol Biol* 426:419–435.
8. Brunger AT (1992) Free R value: A novel statistical quantity for assessing the accuracy of crystal structures. *Nature* 355:472–475.
9. Emsley P, Cowtan K (2004) Coot: Model-building tools for molecular graphics. *Acta Crystallogr D Biol Crystallogr* 60(Pt 12 Pt 1):2126–2132.

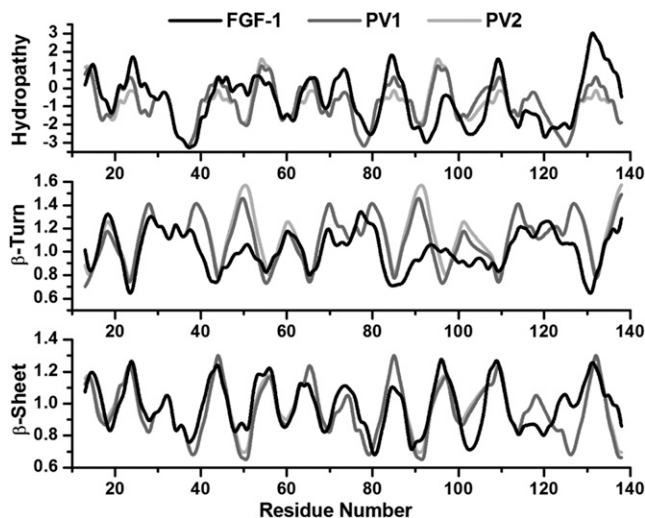


Fig. S1. Hydropathy,  $\beta$ -turn propensity, and  $\beta$ -strand propensity plots for FGF-1, PV1, and PV2 mutant proteins.



**Table S1. Crystallographic data collection and refinement statistics**

	PV1*	PV1 <sup>†</sup>	PV2 <sup>‡</sup>
Space group	P2 <sub>1</sub> 2 <sub>1</sub> 2 <sub>1</sub>	P2 <sub>1</sub> 2 <sub>1</sub> 2 <sub>1</sub>	P2 <sub>1</sub> 2 <sub>1</sub> 2 <sub>1</sub>
Cell constants (Å)			
	a = 38.5	a = 46.7	a = 46.6
	b = 46.6	b = 48.7	b = 48.7
	c = 63.9	c = 67.6	c = 64.9
Maximum resolution (Å)	1.50	1.40	1.90
Mosaicity (°)	0.43	0.40	0.49
Redundancy	6.4	12.8	12.3
Mol/ASU	1	1	1
Matthew coefficient (Å <sup>3</sup> /Da)	1.98	2.65	2.30
Total reflections	120,892	398,211	247,513
Unique reflections	18,903	31,023	12,167
I/σ (overall)	43.4	65.9	38.2
I/σ (highest shell)	6.2	8.0	3.8
Completion overall (%)	99.6	99.9	97.2
Completion highest shell (%)	99.7	99.9	76.2
R <sub>merge</sub> overall (%)	8.0	7.4	9.5
R <sub>merge</sub> highest shell (%)	34.9	30.1	34.2
Nonhydrogen protein atoms	1,009	1,031	974
Solvent molecules/ion	154/10	217/13	177/1
R <sub>cryst</sub> (%)	16.7	18.2	16.5
R <sub>free</sub> (%)	21.1	20.5	21.4
rmsd bond length (Å)	0.006	0.006	0.006
rmsd bond angle (°)	1.08	1.10	1.07
Ramachandran plot			
Most favored (%)	93.5	95.7	100.0
Additional allowed (%)	6.5	4.3	0.0
Generously allowed (%)	0.0	0.0	0.0
Disallowed region (%)	0.0	0.0	0.0
PDB ID code	3Q7W	3Q7X	4D8H

Mol/ASU, molecules per asymmetric unit; I/σ, intensity/standard deviation of intensity (signal-to-noise); R<sub>merge</sub>, agreement among multiple measurements of the same reflection; R<sub>cryst</sub>, crystallographic R index; R<sub>free</sub>, crystallographic R index of the test set.

\*1.5 M (NH<sub>4</sub>)<sub>2</sub>SO<sub>4</sub>, 0.1 M Hepes pH7.4, 0.10 M Li<sub>2</sub>SO<sub>4</sub>.

<sup>†</sup>1.5 M (NH<sub>4</sub>)<sub>2</sub>SO<sub>4</sub>, 0.1 M Tris pH 7.0, 0.10 M Li<sub>2</sub>SO<sub>4</sub>.

<sup>‡</sup>1.5 M (NH<sub>4</sub>)<sub>2</sub>SO<sub>4</sub>, 0.1 M Tris pH 7.0, 0.11 M Li<sub>2</sub>SO<sub>4</sub>.

**Table S2. DSC data for the thermal denaturation of FGF-1, Symfoi-4P, PV1, and PV2 mutant proteins in 0.1 M and 2.0 M NaCl**

Protein	ΔH(T <sub>m</sub> ) (kJ·mol <sup>-1</sup> )	T <sub>m</sub> (°C)	ΔH <sub>van't Hoff</sub> /ΔH <sub>cal</sub>	ΔT <sub>m</sub> 2.0–0.1 M NaCl (°C)
0.1 M NaCl				
FGF-1	PPT			
<i>Symfoi-4P</i> *	599 ± 10	85.0 ± 0.1	1.05 ± 0.07	
PV1	490 ± 3	70.7 ± 0.1	0.96 ± 0.08	
PV2	157 ± 5	34.2 ± 0.2	0.87 ± 0.19	
2.0 M NaCl				
FGF-1	PPT			16.3 <sup>†</sup>
<i>Symfoi-4P</i>	726 ± 2	100.4 ± 0.1	1.13 ± 0.01	15.4
PV1	620 ± 9	88.3 ± 0.2	0.88 ± 0.07	17.6
PV2	357 ± 2	64.5 ± 0.1	0.84 ± 0.04	30.3

H, enthalpy; T<sub>m</sub>, melting temperature; H<sub>van't Hoff</sub>, van't Hoff enthalpy; H<sub>cal</sub>, calorimetric enthalpy; PPT, precipitation.

\*From ref. (4).

<sup>†</sup>Apparent ΔT<sub>m</sub> determined from endotherm peak.